

Interaction induced delocalization of two particles: large system size calculations and dependence on interaction strength

Klaus M. Frahm

Laboratoire de Physique Quantique, UMR C5626 du CNRS, Université Paul Sabatier, F-31062 Toulouse Cedex 4, France,
 e-mail: frahm@irsamc2.ups-tlse.fr

September 14, 1998

Abstract. The localization length L_2 of two interacting particles in a one-dimensional disordered system is studied for very large system sizes by two efficient and accurate variants of the Green function method. The numerical results (at the band center) can be well described by the functional form $L_2 = L_1[0.5 + c(U) L_1]$ where L_1 is the one-particle localization length and the coefficient $c(U) \approx 0.074 |U|/(1 + |U|)$ depends on the strength U of the on-site Hubbard interaction. The Breit-Wigner width or equivalently the (inverse) life time of non-interacting pair states is analytically calculated for small disorder and taking into account the energy dependence of the one-particle localization length. This provides a consistent theoretical explanation of the numerically found U -dependence of $c(U)$.

PACS. 72.15.Rn Quantum localization – 71.30.+h Metal-insulator transitions and other electronic transitions – 72.10.Bg General formulation of transport theory – 71.55.Jv Disordered structures; amorphous and glassy solids

1 Introduction

The quantum eigenstates of non-interacting particles in a random potential are localized if the fluctuations of the potential (the disorder strength) are sufficiently strong (for a review see [1]). This phenomenon of Anderson localization is particularly well understood for one-dimensional or quasi one-dimensional geometries where localization even persists for arbitrarily small disorder strength. For this case efficient numerical methods [1] and also powerful analytical theories in terms of the supersymmetric non-linear σ -model [2,3] and the Fokker-Planck approach for the transfer matrix [3,4] are available.

Dorokhov [5] and, recently, Shepelyansky [6] considered the case of two interacting particles (TIP) moving in a one-dimensional random potential for which they predicted a strong enhancement of the localization length for the pair-states due to the interaction. While the results of Dorokhov are only valid for the case of a strongly attractive interaction confining both particles together, Shepelyansky also considered a local, attractive or repulsive Hubbard interaction. He claimed that among many states with both particles being localized far away, there are a few pairs-states where the typical distance between the particles is of the order of the one-electron localization length L_1 and the center of mass coordinate is characterized by a pair-localization length $L_2 \gg L_1$. Mapping the original problem on a random band-matrix model superimposed with large diagonal elements, he found for the case $L_1 \gg 1$ (length measured in units of the lattice spac-

ing)

$$L_2 \sim \frac{U^2}{t^2} L_1^2 \quad (1)$$

where U is the strength of the Hubbard interaction and t is the value of the hopping matrix element. The disorder strength enters through the value of L_1 (see below). This estimate has been confirmed by Imry [7] using a different argument based on the Thouless scaling block picture [8]. A crucial role is played here by the spreading width Γ (also called Breit-Wigner width) which is the energy scale over which unperturbed states are mixed due to the interaction. Imry identified this energy scale with a generalized Thouless energy defined as the sensitivity of the energy levels with respect to a change of the boundary conditions for a finite block of size L_1 . The pair-localization length is then obtained by scaling theory as $L_2/L_1 = \Gamma/\Delta_2$ where $\Delta_2 \sim t/L_1^2$ is the two-particle level spacing in the finite block. Using an ergodic hypothesis for the one-particle eigenfunctions, one can estimate the spreading width by Fermi's golden rule $\Gamma \sim U^2/(t L_1)$ [6,7,9] reproducing Eq. (1).

First numerical studies in terms of finite size transfer matrix calculations [10] and exact diagonalization [11] confirmed the strong enhancement due to the interaction. Borgonovi et al. [12] showed that the enhancement effect also appears in a related model of two interacting kicked rotors for which it is possible to determine directly the quantum time-evolution. Von Oppen et al. [13] introduced an efficient method to calculate the two-particle Green function and based on their numerical results they pro-

posed the scaling relation $L_2/L_1 \approx 0.5 + 0.054|U|L_1$ with a linear dependence on U contradicting the estimate (1). This behavior was explained by Jacquod et al. [14] who calculated analytically the spreading width for the limit of vanishing disorder. Resumming an infinite series of diagrams they obtained for energies close to the band center $\Gamma/\Delta_2 \sim L_1|U|/\sqrt{t^2 + (U/4)^2}$. Therefore the physical arguments of Refs. [6,7,9] did not contradict the results of [13] but the application of Fermi's golden rule corresponding to lowest order perturbation theory and the ergodic hypothesis appeared to be insufficient to determine Γ .

It is worth mentioning that the topic also inspired considerable progress in the understanding [15,16,17] of the random band matrix model with superimposed diagonal originally introduced and used by Shepelyansky [6]. Furthermore, in Ref. [18], a sophisticated random matrix model was proposed which works for arbitrary space dimension and takes properly both particle coordinates (relative and center of mass coordinate) into account. This model can be mapped onto an effective supermatrix nonlinear σ -model and it is thus possible to explain features like a logarithmically suppressed diffusion or a logarithmically increasing pair size [18] found previously by Borogoni et al. [12] for the pair-diffusive regime in $d > 2$ dimensions where all states are delocalized. Subsequent work was concerned with the role of the level statistics [19] and, very recently, with the fractal structure of the coupling matrix elements due to the interaction [20].

Despite the available evidence in favor for the enhancement effect the general situation is still not really clear, due to different proposals for the dependence of L_2 on W and U [20,21,22] and the claim of Römer et al. that the effect completely vanishes in the limit of infinite system size [23]. This claim, which was contested in [24], is based on the finite size extrapolation of the localization length calculated by a transfer matrix method for finite square samples being put together to an infinite strip.

In this work, we present numerical results (section 2) based on an exact and efficient variant of the Green function method introduced in Ref. [13] that allows to treat rather large system sizes, i. e. $N \geq 1000$. This is indeed important for small disorder values in order to perform an accurate finite size extrapolation. We furthermore present a second variant which consists of the recursive Green function technique applied to an effective band matrix Hamiltonian as considered in [13]. In this approach one can indeed take the limit $N \rightarrow \infty$ and the results we find are consistent with those of the finite size extrapolation of the first variant. The issue of an accurate variant of the Green function method is actually of considerable interest since Römer et al. [23] had questioned the original results of von Oppen et al. due to a certain approximation applied in the original approach of Ref. [13]. We find in our calculations qualitative agreement with those results concerning the strong enhancement of the localization length L_2 and the dependence on L_1 . However, we find nevertheless a quantitative difference concerning the dependence on the interaction strength U which is only linear for sufficiently small U . To understand this, we reconsider the

issue of the determination of the Breit-Wigner width Γ for small disorder (section 3). Improving the Γ estimate of Ref. [14], we can indeed explain the modified U dependence.

Very recently, we learned of related relevant work [25, 26] in which the TIP Green function was evaluated by a decimation method for system sizes up to $N = 251$ [25] or $N = 300$ [26].

2 Numerical Green function approach

We consider two particles in a disordered system interacting via a local Hubbard-interaction and characterized by the following tightbinding Hamiltonian,

$$H = -t \sum_{x,y} \left(|x+1, y\rangle \langle x, y| + |x, y+1\rangle \langle x, y| + \text{h.c.} \right) + \sum_{x,y} \left(\varepsilon(x) + \varepsilon(y) + U \delta_{x,y} \right) |x, y\rangle \langle x, y|. \quad (2)$$

x and y denote the positions of the first and the second particle, respectively. t is the strength of nearest neighbor coupling matrix element which we put to unity in the following and U is the value of the on-site interaction. The disorder energies are random, i. e. $\varepsilon(x) \in [-W/2, W/2]$ with W being the disorder strength. At vanishing interaction $U = 0$ the one-particle eigenstates (at a one-particle energy $E = 0$) are localized with the localization length: $L_1 \approx 105/W^2$ [1]. In this work we do not discuss the particular effects of symmetric or anti-symmetric two-particle states (Bosons or Fermions). The on-site Hubbard interaction only acts on the subspace of symmetric states and our results apply therefore to the case of Bosons. However, for the actual calculations and the representation, we find it more convenient to keep all states.

To determine the two-particle localization length, we consider as in Ref. [13] the two-particle Green function. Since we are interested in the coherent propagation the particles being close, we determine only the Green function matrix elements of doubly occupied states $|xx\rangle$,

$$g_{xy} = \langle xx | (E - H)^{-1} | yy \rangle. \quad (3)$$

A priori, for a finite system of size N , the matrix inverse in (3) has to be evaluated for a $N^2 \times N^2$ matrix. Fortunately, von Oppen et al. [13] have shown that this problem can be reduced to an effective Green function on an N -dimensional space because the interaction operator is proportional to the projector on the space of doubly occupied states. The matrix g in (3) can be calculated [13] from an $N \times N$ -matrix equation

$$g = g_0 \frac{1}{1 - g_0 U}, \quad \text{where } g_0 = g|_{U=0}. \quad (4)$$

The matrix g_0 is given in terms of the one-particle eigenstates $\varphi_\alpha(x)$ and the one-particle energies E_α via,

$$(g_0)_{xy} = \sum_{\alpha,\beta} \varphi_\alpha(x) \varphi_\beta(x) \frac{1}{E - E_\alpha - E_\beta} \varphi_\beta(y) \varphi_\alpha(y). \quad (5)$$

The two-particle localization length L_2 is determined by the exponential decay $g_{x_0,x} \sim \exp(-|x - x_0|/L_2)$ corresponding to

$$\frac{1}{L_2} = - \lim_{N \rightarrow \infty} \frac{1}{N} \left\langle \ln \left| \frac{g_{x,x+N}}{g_{x,x}} \right| \right\rangle. \quad (6)$$

The ensemble average is performed over different disorder realizations and for practical purposes also over some initial sites x close to one boundary. The extra denominator $g_{x,x}$ in (6) is not relevant in the limit $N \rightarrow \infty$ but provides a considerable improvement if (6) is evaluated for finite N . For vanishing interaction, we expect according to (5) $L_2(U = 0) \approx L_1/2$ [13].

In Ref. [13], Eq. (4) was evaluated for a finite system by employing two approximations. First, von Oppen et al. omitted the first factor g_0 and, second, they did not evaluate the full matrix g_0 but only a sufficiently large band on which they applied the recursive Green function technique [27,28] for the matrix inverse in (4). Since g_0 is indeed a band matrix of width $\sim L_1$ both approximations seem to be well justified provided $L_1 < L_2/2$. However, the validity of the corresponding results was seriously questioned by Römer et al. [23] due to these approximations and, furthermore, the limit of very small (vanishing) interaction cannot accurately be studied within this approach.

We have evaluated (4) exactly without any approximations. For this we note two important points concerning the numerical precision and the efficiency. First, the multiplication of the band matrix g_0 with the matrix inverse in (4) requires that the *relative* error of the exponentially small matrix elements of g_0 far away from the diagonal is small [29]. Otherwise, Eq. (6) provides incorrect results for L_2 . This in turn requires that the exponential tails of the $\varphi_\alpha(x)$ are accurate over the whole length scale $x = 1, \dots, N$. According to this, we have determined the one-electron eigenstates by the method of inverse vector iteration [30] which provides the required accuracy by sufficiently increasing the number of iterations. The second point concerns the efficiency. Here the matrix inverse in (4), which costs of the order of N^3 operations, is actually not the limiting factor. This is due to the necessary evaluation of g_0 . The naive application of (5) already costs of the order of N^4 operations. Even though this number can be reduced by exploiting the exponential decay of the $\varphi_\alpha(x)$ this does not yield any significant improvement for small disorder values when $L_1 \sim 50 - 100$. Fortunately, it is possible to determine g_0 exactly with N^3 operations. For this we rewrite (5) in the form

$$(g_0)_{xy} = \sum_{\alpha} \varphi_{\alpha}(x) G_{xy}^{(1)}(E - E_{\alpha}) \varphi_{\alpha}(y), \quad (7)$$

where $G_{xy}^{(1)}(E)$ is the one-particle Green function at energy E that can efficiently be determined by N^2 operations due to the tridiagonal form of the one-electron Hamiltonian. Since this has to be done for N different energies $E - E_{\alpha}$, Eq. (7) provides an algorithm with only N^3 operations.

We have used two variants of the Greens function method. The first is based on a finite size extrapolation (FSE) to

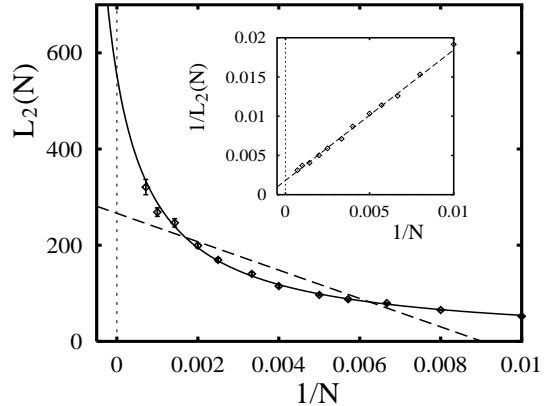


Fig. 1. Finite size two-particle localization length $L_2(N)$ for $U = 1.5$, $E = 0$ and $W = 1.0$ versus $1/N$ ($100 \leq N \leq 1400$). The full curve corresponds to the fit $L_2^{-1}(N) = L_2^{-1} + C/N$ and the dash line corresponds to the fit $L_2(N) = L_2 + \tilde{C}/N$. The insert shows $1/L_2(N)$ versus $1/N$ with the corresponding linear fit.

determine the limit $L_2 = \lim_{N \rightarrow \infty} L_2(N)$. For this, we have calculated the ensemble averaged inverse localization length $L_2^{-1}(N)$ for different system sizes using the exact projected Green function g as given in (4). The limit for $N \rightarrow \infty$ has been determined by the linear fit in $1/N$ of the *inverse* localization length:

$$\frac{1}{L_2(N)} \approx \frac{1}{L_2} + \frac{C}{N}. \quad (8)$$

This ansatz for the finite size extrapolation is highly suggestive from Eq. (6). Assuming, that the typical value of $g_{x,x+N}$ does not depend on N if $N \ll L_2$, we see that (8) reproduces both limits $N \ll L_2$ and $N \gg L_2$.

The quality of the fit is indeed confirmed by the explicit numerical values as can be seen in Fig. 1. For $W = 1.0$ ($L_1 = 105$), $E = 0$, $U = 1.5$, and $100 \leq N \leq 1400$, the fit (8) works quite well while the direct fit $L_2(N) = L_2 + \tilde{C}/N$ is very poor for the considered range of N values. Of course, for $L_2 \ll N$ both extrapolation schemes are equivalent. However, for the case of Fig. 1, L_2 and N are comparable and the choice of the correct method is crucial.

To obtain an independent verification of the extrapolation scheme (8), we have also used a second method which permits to determine L_2 directly for quasi infinite systems. For this, as in Ref. [13], we have omitted the first factor in (4) and replaced in the denominator of the second factor the matrix g_0 by a block-tridiagonal matrix of block size b . This matrix can be viewed as an effective Hamiltonian [13] and it is possible to perform the matrix inverse of (4) by the recursive Green function (RGF) technique [27,28]. In contrast to von Oppen et al., we have applied this method for quasi infinite system size as described in Ref. [27]. The limit (6) can be directly evaluated due to the self averaging behavior of the inverse localization length. The non-vanishing blocks of g_0 are determined in a local approximation, i.e. to calculate

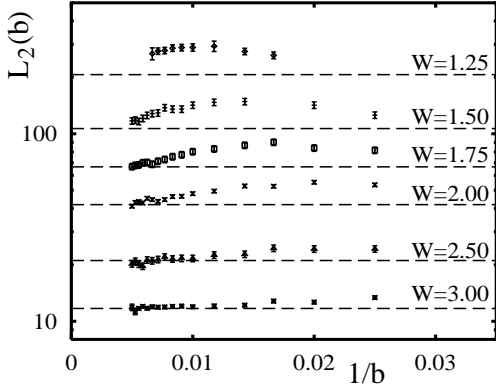


Fig. 2. Localization length $L_2(b)$ (on a logarithmic scale) for $U = 1$ and $E = 0$ obtained by the second method [recursive Green function method applied on (4)] versus the inverse block size $1/b$ ($40 \leq b \leq 200$). The dashed lines correspond to the values of L_2 obtained by the first method (finite size extrapolation).

$(g_0)_{xy}$ for $x, y \in \{x_0 - b + 1, \dots, x_0 + b\}$ we apply Eq. (7) for a finite system of size $N_c > 2b$ containing the sites $x \in \{x_0 - N_c/2 + 1, \dots, x_0 + N_c/2\}$. This works if N_c and b are sufficiently large compared to L_1 because the matrix elements $(g_0)_{xy}$ do not depend on N_c if the sites x, y are far away from the boundaries. For each iteration step of the recursive Green function procedure the disorder realization on the N_c sites is shifted by b sites and g_0 has to be recalculated by (7). We have chosen $N_c = 3b$ and calculated $L_2(b)$ for different values of the block sizes in the interval $40 \leq b \leq 200$. Here, we expect a much faster (exponential) convergence of L_2 as the ratio b/L_1 becomes larger than unity. In Fig. 2, we compare for $U = 1$ and different disorder values, $1.25 \leq W \leq 3.00$, the localization length $L_2(b)$ with the values obtained from the FSE method.

We find overall agreement between both methods and $L_2(b)$ indeed coincides with L_2 for $b \geq b_c \approx 5L_1$. For small disorder values it is quite difficult to arrive at this regime. For $b < b_c$ the values of $L_2(b)$ are typically larger than the values obtained by the first method. To our knowledge, the approach described above is indeed the first method to determine directly the TIP localization length for quasi infinite system size without the side effects of a bag-interaction [6, 10]. This is possible, because the cutoff is applied on an effective Hamiltonian and the neglected matrix elements are indeed exponentially small if the block size b is sufficiently large. The results shown in Fig. 2 provide therefore an additional confirmation of the validity of the above discussed extrapolation scheme.

For a systematic study of the dependence on W and U , we used the first variant based on the FSE scheme (8) which appears to be more efficient, especially for large values of L_1 . For the scope of this paper, we studied the band center $E = 0$ where the localization properties are symmetric with respect to the sign of U . We considered for the disorder values $1.0 \leq W \leq 7.0$ and interaction strengths $0.0 \leq U \leq 2.0$ at least system sizes up to $N = 500$ and

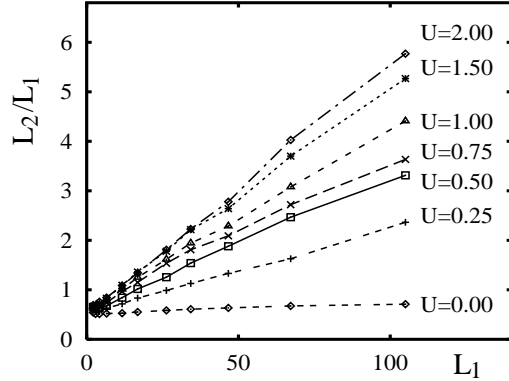


Fig. 3. Enhancement factor L_2/L_1 as a function of $L_1 = 105/W^2$. L_2 is extrapolated as in (8) using system sizes up to $N \leq 1000$. The considered disorder values are $W = 1, 1.25, 1.5, 1.75, 2, 2.5, 3, 4, 5, 6, 7$.

for $W \leq 1.75$ even sizes up to $N = 1000$. (For $W = 1.0$ and $U = 1.5, 2.0$, we have also calculated two data-points with $N = 1400$.) Most of the data points (for the finite size values $L_2(N)$) were determined with a relative error smaller than 2%. For the largest system sizes and smallest disorder values the relative error is 3–3.5%. To verify the scaling relation $L_2/L_1 \approx 0.5 + 0.054|U|L_1$ suggested by von Oppen et al. [13], we show in Fig. 3 the ratio L_2/L_1 as a function of L_1 where L_2 has been obtained by FSE from $L_2(N)$.

The linear behavior in L_1 is qualitatively indeed confirmed but the errors for the smaller disorder values do not allow to exclude a behavior of the type $(L_2/L_1 - 0.5) \propto L_1^\alpha$ with $\alpha < 1$. A corresponding fit indeed gives $\alpha \approx 0.9$ but this depends also on the chosen offset 0.5 (the fit with the offset 0.55 gives $\alpha \approx 1.0$). We mention that the slight deviations from the linear behavior can also be well described by an ansatz of the type $(L_2/L_1 - 0.5) \propto L_1/\ln(CL_1)$ suggested by Borgonovi et al. [12]. However, since the precision of the data does not permit to distinguish significantly between this and the linear behavior, we do not enter into more details here. For $U = 0$, we confirm the previous observation [22, 25] of a slight enhancement $L_2(U = 0)/L_1 \approx 0.5 - 0.7$ which is presumably due to the energy average in Eq. (5) [22, 25].

In Fig. 4, we also show the dependence of L_2 on the disorder strength W (for $U = 1$ and $E = 0$). Previously, Song et al. [22] found a behavior $L_2 \propto W^{-2.9}$ and as we can see the overall slope in Fig. 4 is indeed comparable to this behavior. However, we find for small and large W values significant deviations due to the curvature in the curve of $\ln(L_2)$ versus $\ln(W)$. This is due to the constant term in the above scaling relation. Actually, the data can be extremely well fitted by $L_2 \approx L_1(0.55 + 0.038L_1)$ for the whole interval $1.0 \leq W \leq 7.0$ and one indeed finds the asymptotic behavior $L_2 \propto W^{-4}$ for small W ($L_1 \gg 10$) and $L_2 \propto W^{-2}$ for larger values of W ($1 < L_1 < 10$).

To extract the dependence on U , we determined the slope $c(U)$ in the linear fit $L_2/L_1 = a + c(U)L_1$ which is compared in Fig. 5 with the numerical data. The slope

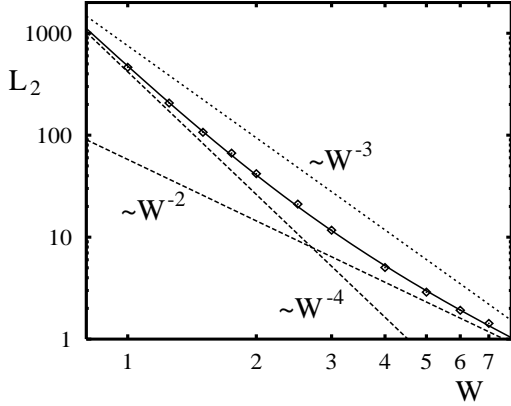


Fig. 4. Dependence of L_2 on W for $U = 1$ (double log-scale). The data-points are the same as in Fig. 3. The full curve is the fit $L_2 = L_1 (0.55 + 0.038 L_1)$ with $L_1 = 105/W^2$. The two dashed lines correspond to the limiting cases $L_2 = 0.038 L_1^2 \propto W^{-4}$ (or $L_2 = 0.55 L_1 \propto W^{-2}$) for $L_1 \gg 10$ ($L_1 \ll 10$). The dotted line corresponds to the behavior $\propto W^{-3}$ for comparison.

$c(U)$ itself is shown in the insert of Fig. 5 as a function of U . Apparently, the U dependence is not linear for the whole interval $0.0 \leq U \leq 2.0$. This linear behavior was observed by v. Oppen et al. [13] for $U \leq 1.0$ where the discrepancy is still quite moderate. At $U = 1.0$ their values are about 40% larger than ours. We believe that this is due to finite size effects and the applied approximations.

Also the estimate $c(U) \propto |U|/\sqrt{1+(U/4)^2}$ based on the analytical calculation of the Breit-Wigner width for $W = 0$ [14] only agrees with the numerical data for sufficiently small U . In the next section, we will try to explain this disagreement and reconsider the determination of the Breit-Wigner width.

3 Breit-Wigner Width and U dependence

The delocalization effect of two interacting particles is related to the finite life time $\tau = \Gamma^{-1}$ of the product states $|\alpha\beta\rangle$ with $\langle x_1 x_2 | \alpha\beta \rangle = \varphi_\alpha(x_1) \varphi_\beta(x_2)$ [6, 7, 9]. The interaction gives rise to transitions $|\alpha\beta\rangle \rightarrow |\gamma\delta\rangle$ which can be viewed as random hops of typical size L_1 . For short time scales when quantum interference effects can be neglected one therefore obtains a diffusive dynamics [6, 9] with the diffusion constant $D \sim L_1^2 \tau^{-1} = L_1^2 \Gamma$. Following a general argument developed in Ref. [31] and applied to the TIP case in Refs. [6, 9], one can estimate the localization length due to quantum interference effects. According to this the classical diffusive behavior is only valid for time scales smaller than the Heisenberg time corresponding to a wave packet of width \sqrt{Dt} , i. e.

$$t < t_H(t) = \nu_{\text{eff}} \sqrt{Dt}. \quad (9)$$

Here ν_{eff} is the density of states per length such that $(L\nu_{\text{eff}})^{-1}$ is the level spacing in a block of size L . For the TIP, we have $\nu_{\text{eff}} \approx \nu_2 L_1$ with $\nu_2(E)$ being the energy

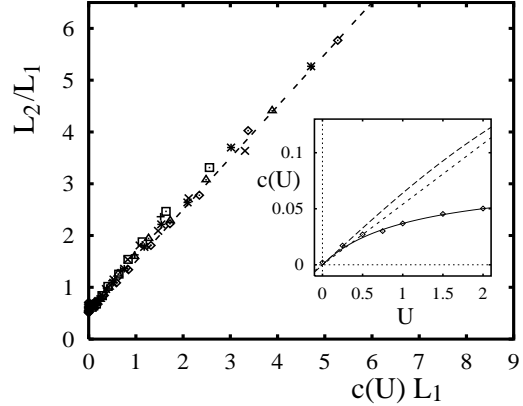


Fig. 5. L_2/L_1 versus the scaling parameter $c(U) L_1$ for the data of Fig. 3 (points) where the quantity $c(U)$ is given by Eq. (23) with $A = 0.028$ and $k_c = 0.25$ (see text). The symbols for the different U values are the same as in Fig. 3. The dashed line corresponds to $L_2/L_1 = 0.5 + c(U) L_1$. The insert shows $c(U)$ as a function of U . The data points are the values obtained as the slope in the fit $L_2/L_1 = a + c(U) L_1$. The full line is the analytical expression (23) (same values for A and k_c as above), the dotted line is the linear dependence $0.054 U$ found in Ref. [13] and the dashed line is the dependence suggested in Ref. [14].

dependent two-particle density of states. $\nu_2(E)$ is proportional to the inverse bandwidth $1/(8 + 2W) \sim 1$ with a logarithmic singularity at the band center (for $W = 0$). The density ν_{eff} corresponds to the number of well coupled pair states with the same center of mass coordinate but with different relative coordinates (up to a maximal value $\sim L_1$).

At $t \approx t_c = \nu_{\text{eff}}^2 D$, when the condition (9) ceases to be valid, the discrete energy spectrum can be resolved and localization with a localization length $L_2 \sim \sqrt{Dt_c} \sim \nu_{\text{eff}} D$ sets in. This general relation for quasi 1d systems has also been obtained in a more rigorous way using the supersymmetric non-linear σ -model [2]. In view of this, the Breit-Wigner width Γ and L_2 are related by

$$L_2 \sim \nu_{\text{eff}} D \sim L_1^3 \Gamma \nu_2. \quad (10)$$

Jacquod et al. [14] determined Γ using diagrammatic perturbation theory (in U) for the case of vanishing disorder, $W = 0$, and finite system size N . They argued that one obtains a good estimate of Γ for finite W by replacing N with L_1 due to the ballistic dynamics in 1d for length scales up to L_1 . For energies close to the band center and moderate interaction strengths $U \lesssim 1$, their result reads

$$L_2 \sim L_1^2 \frac{|U|}{\sqrt{1+(U/4)^4}}. \quad (11)$$

As we can see in the insert of Fig. 5 our numerical data agrees with this behavior only for very small values of U . We therefore feel that it is justified to reconsider the issue of the Breit-Wigner width which can be calculated from

the energy dependent local density of states

$$\rho_{\alpha\beta}(E) = -\frac{1}{\pi} \text{Im} \langle \alpha\beta | (E + i0 - H)^{-1} | \alpha\beta \rangle, \quad (12)$$

with $|\alpha\beta\rangle$ as above. Using Schur's formula to perform the matrix inverse, we rewrite (12) as

$$\rho_{\alpha\beta}(E) = -\frac{1}{\pi} \text{Im} \left[E + i0 - E_\alpha - E_\beta - \langle \alpha\beta | \hat{U} | \alpha\beta \rangle + \Gamma_{\alpha\beta}/2 \right]^{-1}, \quad (13)$$

$$\begin{aligned} \Gamma_{\alpha\beta} &= \Gamma_{\alpha\beta}^{(0)} + i \Gamma_{\alpha\beta}^{(1)} \\ &= -2 \langle \alpha\beta | \hat{U} (E + i0 - \tilde{H}) \hat{U} | \alpha\beta \rangle. \end{aligned} \quad (14)$$

Here $\hat{U} = U \sum_x |xx\rangle\langle xx|$ is the interaction operator and $\tilde{H} = \tilde{P} H \tilde{P}$ with the projector $\tilde{P} = 1 - |\alpha\beta\rangle\langle\alpha\beta|$. Eq. (13) corresponds to the Lorentzian or Breit-Wigner form of the local density of states provided that the energy dependence of $\Gamma_{\alpha\beta}$ is weak. The imaginary part $\Gamma_{\alpha\beta}^{(1)}$ is the width of the Lorentzian. In the following, we replace \tilde{H} by H , and we first evaluate (14) for the case of vanishing disorder. For this we only need the projected Green function (3) due to the appearance of \hat{U} in (14). In view of Eq. (4), we first determine

$$\begin{aligned} (g_0)_{xy} &= \langle xx | (E + i0 - H_0)^{-1} | yy \rangle \\ &\approx \frac{1}{2\pi} \int_{-\pi}^{\pi} dk e^{ik(x-y)} \tilde{g}_0(k) \end{aligned} \quad (15)$$

with

$$\begin{aligned} \tilde{g}_0(k) &= \frac{1}{2\pi} \int_{-\pi}^{\pi} dq \frac{1}{E + i0 + 2[\cos(q) + \cos(k-q)]} \\ &= -i \frac{1}{\sqrt{4 \cos^2(k/2) - E^2}}. \end{aligned} \quad (16)$$

The Green function at $W = 0$ and $U \neq 0$ is then given by

$$g_{xy} = \frac{1}{2\pi} \int_{-\pi}^{\pi} dk e^{ik(x-y)} \frac{\tilde{g}_0(k)}{1 - U \tilde{g}_0(k)}. \quad (17)$$

From this and Eq. (14), we obtain

$$\Gamma_{\alpha\beta} = -2U^2 \sum_{x,y} \varphi_\alpha^*(x) \varphi_\beta^*(x) g_{xy} \varphi_\alpha(y) \varphi_\beta(y). \quad (18)$$

Inserting the plane wave eigenstates for φ_α or φ_β , we exactly recover the result of Ref. [14] for the Breit-Wigner width. This shows that the diagrammatic approach of [14] is equivalent to our above approximations (replacing \tilde{H} by H and continuum limit for k).

The generalization to the disordered case essentially gives rise to two modifications. Using diagrammatic perturbation theory in the disorder, one can first evaluate the average of the Green functions (15) and (16) which amounts to the replacement $E + i0 \rightarrow E + i\gamma$ where γ is determined by a Dyson equation. For weak disorder one finds $\gamma \sim W^2$ (with eventual logarithmic corrections at

the band center). In the following discussion, we neglect the effect of this small γ which essentially regularizes (16) at the singularity. The second, more important, modification due to finite disorder concerns the eigenfunctions $\varphi_\alpha(x)$ in Eq. (18). Here the energy dependence of the one particle localization length plays an important role. To see this, we use the toy ansatz

$$\varphi_\alpha(x) \approx \frac{1}{\sqrt{L_{1,\alpha}}} e^{-|x-x_\alpha|/L_{1,\alpha} + i k_\alpha x} \quad (19)$$

with $E_\alpha = -2 \cos k_\alpha$ and an energy dependent localization length $L_{1,\alpha} \approx L_1 \sin^2(k_\alpha)$ [1]. This ansatz essentially corresponds to a particle moving ballistically with a well defined momentum inside the localization domain around x_α . This is indeed reasonable because in one dimension the mean free path is of the same order as the localization length. However, the momentum has to be larger than its typical uncertainty, i. e. $|k_\alpha| \gtrsim \Delta k \sim L_{1,\alpha}^{-1}$. Therefore the ansatz (19) is valid for momenta with $|\sin k_\alpha| \gtrsim L_1^{-1/3}$ corresponding to energies not being close to the band center. Inserting (19) in (18) and choosing $x_\alpha \approx x_\beta$, we obtain

$$\Gamma_{\alpha\beta} \approx -2U^2 \frac{1}{L_{1,\alpha} + L_{2,\alpha}} \frac{\tilde{g}_0(k_\alpha + k_\beta)}{1 - U \tilde{g}_0(k_\alpha + k_\beta)} \quad (20)$$

giving rise to the Breit-Wigner width (for $E = 0$)

$$\Gamma_{\alpha\beta}^{(1)} \approx \frac{U^2/(4L_1)}{\sin^2 k_\alpha + \sin^2 k_\beta} \frac{|\cos[(k_\alpha + k_\beta)/2]|}{\cos^2[(k_\alpha + k_\beta)/2] + (U/4)^2}. \quad (21)$$

These expressions differ by the k -dependent localization length from the result of Ref. [14]. Since $\Gamma_{\alpha\beta}^{(1)}$ depends strongly on the momenta k_α and k_β , we determine the average with respect to these momenta [14]:

$$\Gamma = \frac{1}{4\pi^2} \int_{-\pi}^{\pi} dk_\alpha \int_{-\pi}^{\pi} dk_\beta \delta(E - E_\alpha - E_\beta) / \nu_2(E). \quad (22)$$

Using Eq. (10), relating Γ with L_2 , we can estimate for $E \rightarrow 0$ the two particle localization length as

$$\begin{aligned} L_2 &\approx c(U) L_1^2, \\ c(U) &= A \frac{2}{\pi^2} \int_0^\pi dk \frac{1}{(\sin^2 k + k_c^2)} \frac{(U/4)^2}{\sin^2 k + (U/4)^2} \\ &= \frac{2A|U|}{\pi k_c} \frac{s(\frac{U}{4}) + k_c^2}{|U| s(\frac{U}{4}) \sqrt{s(k_c)} + 4k_c s(k_c) \sqrt{s(\frac{U}{4})}} \end{aligned} \quad (23)$$

where $s(x) = 1 + x^2$, A is a numerical prefactor and k_c is a cutoff value to regularize the integral for small k where the ballistic ansatz (19) is invalid. For the values $k_c = 0.25$ and $A = 0.028$ the U -dependence of (23) fits very well the numerical data for the slope $c(U)$ which can be seen in Fig. 5. We can considerably simplify the somewhat lengthy expression (23) by neglecting the quadratic corrections U^2 and k_c^2 and slightly modifying A ,

$$c(U) \approx 0.074 \frac{|U|}{|U| + 1}. \quad (24)$$

This approximation is numerically very accurate with an relative error smaller than 1 % for $0 \leq |U| \leq 2.0$. The linear behavior of $c(U)$ for small $|U|$ is due to a combination of the logarithmic singularity in the density of states at $E \rightarrow 0$ and of large values of $\Gamma_{\alpha\beta}^{(1)} \sim U$ if $\cos[(k_\alpha + k_\beta)/2] \approx \pm U$.

In view of the agreement between the numerical data and the theoretical estimate for $c(U)$, we conclude that the idea of diffusively moving particle pairs for short time scales finally becoming localized due to quantum interference [6, 7, 9, 14] can indeed quantitatively explain the delocalization effect. For this it is important to evaluate carefully the Breit-Wigner width by taking into account the energy dependence of the one particle localization length.

Despite this agreement we want to emphasize that the result (23) is nevertheless based on several qualitative arguments. Actually, the application of the relation (10) is somewhat problematic because both the Breit-Wigner width and the one-particle localization length do not have unique values due to their energy dependence. It is a priori not clear if the simple average (22) is really sufficient and accurate. Furthermore, Eqs. (23), (24) depend on the artificial cutoff parameter k_c . Theoretically, we expect that $k_c \sim L_1^{-1/3}$ because of the invalidity of the ballistic ansatz (19) for small momenta $|k| < k_c$. Numerically, the case $k_c = 0.25$ indeed corresponds to $L_1 \approx 50 - 100$ the largest considered L_1 values. However, the resulting dependence on L_1 , i. e. $L_2 \sim L_1^{7/3}$ clearly disagrees with the numerical data. We attribute this to the fact that for small momenta according to $L_{1,\alpha} \approx L_1 \sin^2 k_\alpha$ the effective size of the random hops is strongly reduced. This feature is not properly taken into account in the relation (10). Therefore it would be interesting to carefully generalize this relation to the case where Γ and L_1 have complicated distributions instead of unique values.

4 Conclusion

In this work, we have presented and applied two new accurate and efficient variants of the Greens function method originally introduced by von Oppen et al. [13] to study the TIP localization problem [6]. Our results for the TIP localization length L_2 can be well fitted (Fig. 5) by the functional form $L_2 = L_1[0.5 + c(U) L_1]$. The behavior of the slope $c(U) \approx 0.074|U|/(1 + |U|)$ is determined by the U -dependence of the Breit-Wigner width Γ of non-interacting pair states. For this we presented an accurate estimate of Γ extending former work of Jacquod et al. [14].

We think that our results provide important additional evidence for the delocalization effect as such. In particular, we find for $U = 2.0$ and $W = 1.0$ an enhancement factor $L_2/(2L_1) \approx 11.5$. Our data is in qualitative agreement with former results of Song et al. [22], who directly used the less efficient recursive Green function technique for smaller system sizes ($N \leq 200$), and with very recent work [25, 26] based on the decimation method ($N \leq 251$ and $N \leq 300$). In view of this the original claim of Römer et

al. [23] that there is no delocalization effect for infinite system size can no longer be maintained. To understand the transfer matrix data on which this claim was based, we remind that the considered disorder value $W = 3.0$ was relatively large such that L_2 and L_1 are nearly equal. Using, the Green function method one can still measure the enhancement because $L_2 > L_1/2$. However, in the transfer matrix approach there is a direct competition of L_2 with L_1 [26]. Furthermore, even for smaller disorder, the finite size behavior of the transmission eigenvalues is very subtle and one has to be careful about the finite size extrapolation here [32].

While the delocalization effect is now well established, the situation is less clear concerning the functional dependence of L_2 on L_1 . The formerly observed powerlaw $L_2 \sim L_1^\alpha$ with $\alpha \approx 1.45 - 1.65$ [10, 22, 25] was obtained by a fit ansatz without constant term. According to our above discussion (see Fig. 4) it is numerically not obvious to distinguish this powerlaw from the functional form we proposed above. Waintal et al. [20] gave an argument in favor of the former with $\alpha = 1.5$. This argument is based on the multifractal properties of the interaction induced coupling matrix elements in combination with an estimate of Γ using Fermi's golden rule. We believe that this analysis is indeed important and very relevant to the problem. Actually, our result (21) for the Breit-Wigner width contains a strong dependence on the initial one-particle states due to partial momentum conservation. This leads to strong fluctuations of Γ which are presumably directly related to the multifractal statistics of the coupling matrix elements. However, the analytical calculations of Ref. [14] and of section 3 clearly show that the simple application of Fermi's golden rule is not sufficient and the numerical data do not show the corresponding behavior $L_2 \sim U^2$. To understand these issues in more detail further work is necessary.

We emphasize that our numerical data and the estimate (23) are valid for moderate interaction strengths $|U| \leq 2.0$. For larger values of U one expects that L_2 will be reduced due to the particular projector structure of the interaction operator \hat{U} . Waintal et al. [20] presented a duality transformation mapping the case of $|U| \gg 1$ to a similar problem with $|U| \ll 1$ and a different reference basis. According to this $L_2(U)$ should obey the duality relation $L_2(U) \approx L_2(\sqrt{24}/U)$ [20].

Finally, we mention that the numerical trick to evaluate efficiently the matrix g_0 via Eq. (7) also works in higher dimensions, even though the gain is less spectacular. In d dimensions and a system of total size (volume) N one can calculate $G^{(1)}(E)$ by the recursive Green function method which provides an algorithm to evaluate (7) with $N^{3+(d-1)/d}$ operations. In particular the case of two dimensions is important due to recent claims of Ortuno et al. and Cuevas [33] for a delocalization transition for two interacting particles in $d = 2$. We think it is necessary to consider larger system sizes as in Ref. [33] in order to decide whether there is a real transition or a very strong delocalization with a finite but very large two-particle localization length as it was argued by Shepelyansky [9].

The author thanks Dima Shepelyansky and Bertrand Georgeot for inspiring discussions. The Aspen Center for Physics is acknowledged for its hospitality during the workshop Quantum Chaos and Mesoscopic Systems at which a part of this work was done.

References

1. B. Kramer and A. MacKinnon, Rep. Prog. Phys. **56**, 1469 (1993).
2. K. B. Efetov, *Supersymmetry in Disorder and Chaos*, Cambridge University Press (1997).
3. T. Guhr, A. Müller-Groeling, and H. A. Weidenmüller, Phys. Rep. **299**, 189 (1998).
4. C. W. J. Beenakker, Rev. Mod. Phys. **69**, 731 (1997).
5. O. N. Dorokhov, Zh. Eksp. Teor. Fiz. **98**, 646 (1990) [Sov. Phys. JETP **71**, 360 (1990)].
6. D. L. Shepelyansky, Phys. Rev. Lett. **73**, 2607 (1994).
7. Y. Imry, Europhys. Lett. **30**, 405 (1995).
8. D. C. Thouless, Phys. Rev. Lett. **39**, 1167 (1977).
9. D. L. Shepelyansky, Proceedings of les Rencontres de Moriond 1996 on “Correlated Fermions and Transport in Mesoscopic Systems”, edited by T. Martin, G. Montambaux and J. Trân Thanh Vân, 201 (1996).
10. K. Frahm, A. Müller-Groeling, J.-L. Pichard, and D. Weinmann, Europhys. Lett. **31**, 169 (1995).
11. D. Weinmann, A. Müller-Groeling, J.-L. Pichard, and K. Frahm, Phys. Rev. Lett. **75**, 1598 (1995).
12. F. Borgonovi and D. L. Shepelyansky, Nonlinearity **8**, 877 (1995); J. Phys. I France **6**, 287 (1996).
13. F. von Oppen, T. Wettig, and J. Müller, Phys. Rev. Lett. **76**, 491 (1996).
14. Ph. Jacquod, D. L. Shepelyansky, and O. P. Sushkov, Phys. Rev. Lett. **78**, 923 (1997).
15. P. Jacquod and D. L. Shepelyansky, Phys. Rev. Lett. **75**, 3501 (1995).
16. Y. V. Fyodorov and A. D. Mirlin, Phys. Rev. B **52**, R11580 (1995).
17. K. Frahm and A. Müller-Groeling, Europhys. Lett. **32**, 385 (1995).
18. K. Frahm, A. Müller-Groeling, and J.-L. Pichard, Phys. Rev. Lett. **76**, 1509 (1996); Z. Phys. B **102**, 261 (1997).
19. D. Weinmann, J.-L. Pichard, Phys. Rev. Lett. **77**, 1556 (1996).
20. X. Waintal, and J.-L. Pichard, preprint (1997, cond-mat/9706258); X. Waintal, D. Weinmann, and J.-L. Pichard, preprint (1998, cond-mat/9801134); S. D. T. Arias, X. Waintal, and J.-L. Pichard, (1998, cond-mat/9808136)
21. I. V. Ponomarev and P. G. Silvestrov, Phys. Rev. B **56**, 3742 (1997).
22. P. H. Song and Doochul Kim, Phys. Rev. B **56**, 12217 (1997).
23. R.A. Römer and M. Schreiber, Phys. Rev. Lett. **78**, 515 (1997); *ibid.* **78**, 4890 (1997).
24. K. M. Frahm, A. Müller-Groeling, J.-L. Pichard and D. Weinmann, Phys. Rev. Lett. **78**, 4889 (1997).
25. M. Leadbeater, R. A. Römer, and M. Schreiber, preprint (1998, cond-mat/9806255 and cond-mat/9806350).
26. P. H. Song and F. v. Oppen, preprint (1998, cond-mat/9806303).
27. A. MacKinnon, J. Phys. C **13**, L1031 (1980); Z. Phys. B **59**, 385 (1985).
28. B. Huckestein, Rev. Mod. Phys. **67**, 357 (1995).
29. A uniform *absolute* numerical error of the order of the machine precision $\sim 10^{-16}$ is *not sufficient* due to exponentially small matrix elements.
30. H. R. Schwartz, *Numerische Mathematik*, B. G. Teubner, Stuttgart (1986).
31. B. V. Chirikov, F. M. Izrailev, and D. L. Shepelyansky, Sov. Scient. Rev. (Gordon & Bridge) **2C**, 209 (1981); *ibid* Physica D **33**, 77 (1988).
32. K. M. Frahm and A. Müller-Groeling, in preparation.
33. M. Ortuno and E. Cuevas, preprint (1998, cond-mat/9808104); E. Cuevas, preprint (1998, cond-mat/9808139).